

Intelligent Sliding Mode Control Under Maximum Power Point Tracking with Indirect Speed Controller Strategy for Mechanical Wind Turbine System

Bechir Fatnassi¹, Borhen Torchani¹, Anis Sellami¹ and Germain Garcia²

¹ Electrical engineering Department, University of Tunis,
ENSIT, LISIER Laboratory Tunis, Tunisia

² Laboratoire LAAS-CNRS, Université de Toulouse
CNRS, INSA, Toulouse, France

*Corresponding author; Email: fbechir.76@gmail.com

Article Info

Article history:

Received , 17/06/2025

Revised , 28/07/2025

Accepted , 06/08/2025

Keywords:

Wind Turbine ;
Maximum Power Point Tracking (MPPT);
Indirect Speed Controller (ISC);
Artificial neural network (ANN);
Sliding mode controller (SMC);

ABSTRACT

This paper introduces an advanced sliding mode control (SMC) approach integrated with a maximum power point tracking (MPPT) strategy, designed for two-mass variable speed wind turbine (VSWT) systems. The method employs an indirect speed controller (ISC) to set the reference electromagnetic torque based on the turbine's maximum power curve. However, the close coupling between electromagnetic torque (T_{em}) and rotational speed (Ω_m) in the ISC limits dynamic flexibility, leading to slower system responses due to mechanical coupling effects. To address this, the proposed ANN-SMC model leverages the robustness of SMC and the adaptability of artificial neural networks (ANN) to enhance decoupling between T_{em} and Ω_m . This ensures optimal performance even in uncertain conditions. The experiment will be conducted on three types of wind conditions: steady, turbulent, and gusty. Simulation results in Matlab/Simulink validate the model's effectiveness in meeting dynamic performance goals.

I. Introduction

Since it taps into a free, abundant source of electricity, renewable energy has positive externalities on a global scale. Moreover, it significantly reduces greenhouse gas emissions compared to traditional energy generation, contributing to climate change mitigation. It also lessens dependence on resource imports. In fact, with the rapid expansion of the renewable energy market worldwide, carbon neutrality targets for 2050 now seem achievable.

In recent years, wind energy has become the most prevalent renewable resource because it can be installed on a large scale and in various locations worldwide. Its non-polluting nature, combined with significant economic and ecological benefits, has contributed to its widespread adoption [1]. As a result, by 2024, the global installed capacity of wind power exceeded 1 terawatt (1,021 gigawatts), representing a major milestone for the industry. This achievement reflects a 13% increase from the previous year, driven by a record addition of 117 gigawatts of new capacity in 2023 (Global Wind Energy Council) (RenouVolt). The growth has been particularly notable in

China, the United States, Brazil, Germany, and India, which together accounted for a substantial portion of the new installations (Global Wind Energy Council) (RenouVolt).

The mechanical modelling of a wind turbine is complex. There are many mechanical components and forces experienced or transmitted through its elements. It is therefore necessary to select the dynamics to be represented and the typical values of their characteristic parameters. Wind speed is random and instable with significant fluctuations that cause mechanical loads on the structures of the aero-turbine, leading to damage to its structures (Steevens and Flect, 2004; Yeh et al., 2015; V. Petrović, M. Jelavić, 2015; M.Kao and C.Wang,2017; A.E. Yaakoubi and K. Attari, 2018) [2], [3], [4], [5] and [6] resulting in power output oscillations. The Maximum Power Point Tracking (MPPT) control strategy plays an important role in this, and responsible for real-time regulation of actual wind scenario, at this time adapting the operating point through varying to increase capturing energy over a wide range of speeds with these adjustments.

As shown in Figure 1, there are four working regions according to different wind conditions (A.D. Wright, L. Fingersh,2008; Ahmad. M.,2017; X. Zhang, J.jia,2022;J.Xie and H. Dong,2023)[7], [8], [9] and [10]. Region1 corresponds to cut-in wind speed. In region2, the algorithm of maximum power point tracking is implemented in order to extract as much power as possible. In region3 the power generation is at the rated level so a pitch control is employed in order to reduce mechanical loads. Region 4 corresponds to cut-out wind speed; the power is kept constant. In this paper, the study of the MPPT algorithm consists of region 2.

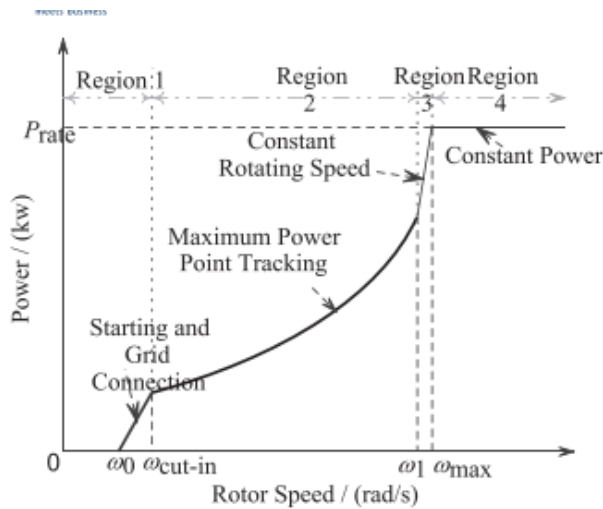


Figure.1 Wind turbine control mode in different regions

There are a lot of studies about the different MPPT strategies, such as TSR control which compares the real value of Tip Speed Ratio (TSR) with the optimal one (Cardenas R, Pena R,2004) [11]. Perturb and Observe (PO) control is used to decide search direction and step size of rotation speed via changes in generator output. (Datta. R and, Ranganathan,2003; H.Mousa and A.Youssef 2021; Barakati et al,2018; X. Zhang, J.jia,2022; J. Xie and H. Dong,2023). [9], [12] and [13].

Optimal torque (OT) control is simple, easy to implement and have a stable torque regulation don't need a measurement of wind speed (Morimoto S. and Nakayama H.,2005; Koutroulis E and Kalaitzakis K.,2006; Hussein M and Senjyu T,2013; Martyanov AS, Troickiy AO., 2018). [14], [15], [16] and [17]. The problem is that these traditional MPPT methods work well only under certain conditions and they fail to deal with the nonlinear and quickly changing dynamics of wind energy systems, so recent research suggests that classical control do not provide better performance than other controllers such as intelligent algorithm and hybrid method.

Hybrid controllers combine different maximum power point tracking (MPPT) techniques (Wang.Q. and Chang L.,2004; Hong MK, Lee H, 2010; Kazmi SMR, Goto H., 2011; You X, Zhou B.,2012; Lalouni et al.,2015; Li, B.and Tang, W.,2017; Pande, J.; Nasikkar, P.,2021) [18], [19], [20], [21], [22] and [23] or a general network control method (such as proportional integral derivative or PID) combined with an algorithm. With advanced technologies (e.g. fuzzy logic, neural systems, etc.) or machine learning (Pucci M, Cirrincione M.,2011;A.E.

Yaakoubi et al,2019; Xie, Jingjie & Dong, Hongyang,2023) [10], [24] and [25] this combination allows the controller to adapt to different operating conditions more efficiently. It provides better performance, stability, and durability than using only one control method because wind energy system has nonlinear characteristics, highly coupled internal variables with swift fluctuation Moreover.

The robust feature of Sliding Mode Control (SMC) regarding system uncertainties and external disturbances motivates its use in wind turbine control, much research has been proposed in this context (Ammar et al.,2019; Berrada et al., 2020;H.Chojaa, A.Derouich,2021; Bu-Lai W, Zi-Xin,2023; Padmanabhuni & Nishanth 2023; Torchani et al, 2024).[26], [27], [28], [29], [30] and [31]. The foundational research on SMC was initially carried out by Soviet control theorists (Petrov et al., 1964; Itkis, 1976; Zinober, 1994). [32], [33] and [34].

This paper provides a description of the developing process and an SMC Approach for Mechanical Wind Turbines supported by ANN-based MPPT system. The ANN generates precision reference triggers for torque T_{em}^* and rotor speed Ω_m^* from historical data of wind speed of wind farm site sidi DAOUED ALHAOUARIA TUNISIA, which is then used by the SMC to maintain the optimal performance. The integration is intended to marry the predictive capabilities of ANNs and the robust control properties of SMC, hence, making sure that the turbine operates at its best under different wind conditions.

By means of thorough analysis, both theoretical development and simulations, and practical validations, the study intends to show the effectiveness of the idea of hybrid control. The results show that energetic efficiency and system resilience were significantly improved, there by bringing forth the possibilities.

This paper describes an advanced control method integrating Sliding Mode Control (SMC) with Maximum Power Point Tracking (MPPT) for two-mass Variable Speed Wind Turbine (VSWT) mechanical systems. The approach uses an Indirect Speed Controller (ISC) that calculates the reference electromagnetic torque based on the maximum power curve, capitalizing on the VSWT's stable dynamics near this operating region. However, while the ISC simplifies the control strategy, it has a key limitation: it creates a tight coupling between the electromagnetic torque (T_{em}) and the rotational speed (Ω_m), leading to slow response due to the system's mechanical coupling dynamics.

To address this issue, the paper proposes a solution combining Artificial Neural Networks (ANN) with Sliding Mode Control (SMC), which offers the benefits of both robust control from SMC and the adaptability and learning capabilities of ANN. This hybrid ANN-SMC model dynamically decouples T_{em} and Ω_m , enabling faster and more optimal system response even when faced with uncertainties or disturbances.

The model's effectiveness is demonstrated through simulations conducted in Matlab/Simulink, showing that the control system meets the desired dynamic performance criteria under specific operating conditions.

II. Wind turbine model

The wind turbine consists of the aerodynamic part which transforms the kinetic energy of the wind into mechanical energy in the form of rotation of the shaft linked to the rotor, the gearbox which is generally an epicyclic gear train which multiplies the rotation speed, (Fig.2) a generator which converts the mechanical energy into electrical energy and rotor- and grid-side converters. The electrical power produced will be injected into the grid (Y. Mousavi, G.Bevan,2022) [35].

II.1. Aerodynamic Model

The aerodynamic model characterizes the rotor's process of extracting power from the wind(Zheng et al.,2009,Torchani et al, 2024) [31] and [36],where the mechanical torque is determined by the interaction of airflow with the blades so he evaluates the turbine torque T_t as a function of wind speed V_v and the turbine angular speed Ω_t presented in Fig. 3 and Fig. 4.

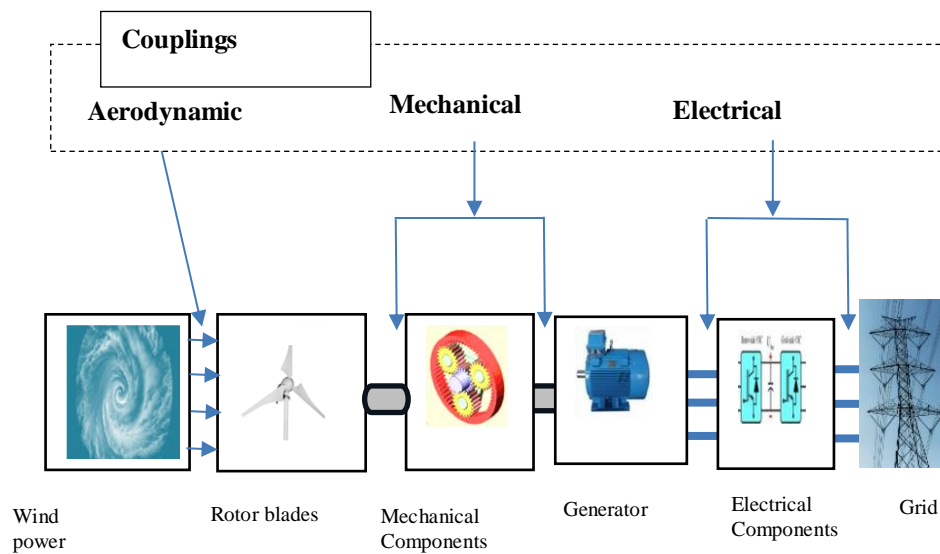


Figure.2 General block diagram of wind energy conversion systems

To calculate the torque on the low-speed shaft, the wind speed is approximated as the average wind speed across the swept area of the blades. The kinetic energy of the wind moving at velocity (V) across a surface area (A) is given by the following expression:

$$P_{vent} = \frac{1}{2} \rho A V^3 \quad (1)$$

Where ρ is the air density.

The wind turbine can recover only a part of that power:

$$P_t = \frac{1}{2} \rho \pi R^2 C_p(\lambda, \beta) V_v^3 \quad (2)$$

where R denotes the radius of the wind turbine and C_p is the power coefficient, a dimensionless parameter that quantifies the efficiency of the wind turbine in converting the wind's kinetic energy into mechanical energy. For a specific wind turbine, this coefficient depends on factors such as wind speed, the rotational speed of the turbine, and the pitch angle of the blades.

The power coefficient C_p is always less than or equal to the Betz limit (~59.3%), (Freris,1990) [37] which is the theoretical maximum efficiency for wind turbine.

C_p is often given as a function of the tip speed ratio, λ , defined by:

$$C_p = \frac{P_t}{P_{vent}} \quad (3)$$

$$\lambda = \frac{R \Omega_t}{V_v} \quad (4)$$

Where Ω_t is the angular speed of the rotor.

The torque generated by the rotor is derived from the power absorbed and the rotational speed of the turbine:

$$T_t = \frac{P_t}{\Omega_t} = \frac{\pi}{2\lambda} \rho R^3 C_p(\lambda, \beta) V_v^2 \quad (5)$$

The simplest method to represent the torque and power coefficient C_p is through analytical expressions based on the tip speed ratio (λ) and the pitch angle (β). A commonly used and easily adaptable expression for various turbines is:

$$C_{p(\lambda,\beta)} = A_1\left(\frac{A_2}{\lambda'} - A_3\beta - A_4\right) \cdot e^{\frac{A_5}{\lambda'}} + A_6$$

$$\frac{1}{\lambda'} = \frac{1}{\lambda + 0.08 \cdot \beta} - \frac{0.035}{\beta^3 + 1}$$

Simulation of Cp with Matlab/ Simulink

Avec : A1= 0.5, A2= 116, A3= 0.4, A4=5, A5 = -21 et A6 = 0.0068

Figure3 obtained represents the variation in aerodynamic efficiency Cp as a function of β and λ .

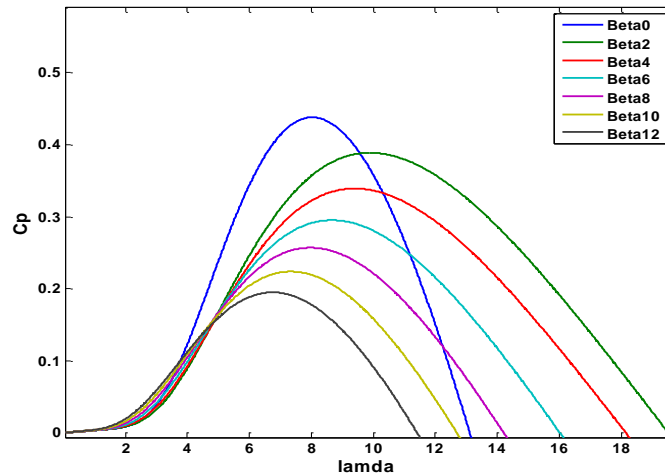


Figure 3. Power coefficient Cp (λ, β)

II.2. Mechanical Model

In this section we are interested in the description and modeling of the mechanical part of the wind turbine which is essentially constituted by the turbine (3 blades mounted on a shaft) and the gearbox. We consider that it is a two-mass system which represent the wind turbine and the generator. On the left side is the low-speed shaft Ω_{t-ar} linked to the turbine with a high torque T_{t-ar} and on the right side is the high-speed shaft Ω_m linked to the generator shaft by means of a coupling with a low transmissible torque T_{em} , to connect these two parts a flexible shaft is mounted.

D_t and D_m are the friction coefficients, representing the mechanical losses due to friction in the rotational movement.

The inertia J_t pertains to the masses on the turbine side, while J_m pertains to those of the electrical machine.

The stiffness and damping coefficients, K_m and D_{tm} , characterize the flexible coupling between the two inertias. (Figure.4)

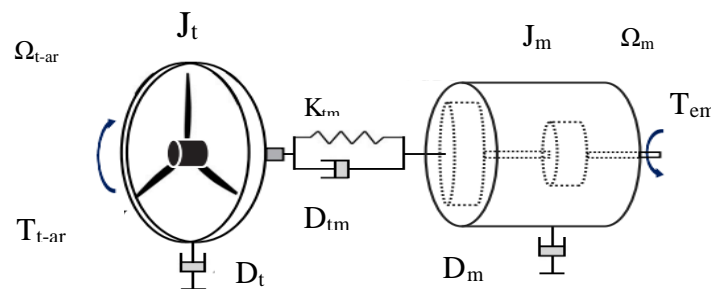


Figure.4 Schematic diagram of a two-mass drivetrain

The turbine's rotational speed and driving torque are represented on the high-speed shaft as follows:

$$\Omega_m = N\Omega_t \quad (6)$$

- Equation of the first mass:

$$J_t \frac{d\Omega_{t-ar}}{dt} = T_{t-ar} - D_t\Omega_{t-ar} - T_{em} \quad (7)$$

- Second mass equation:

$$J_m \frac{d\Omega_m}{dt} = T_{em} - D_m\Omega_m \quad (8)$$

- Dynamics of the electromagnetic torque:

$$\frac{dT_{em}}{dt} = K_{tm}(\Omega_{t-ar} - \Omega_m) + D_m\left(\frac{d\Omega_{t-ar}}{dt} - \frac{d\Omega_m}{dt}\right) \quad (9)$$

III. Indirect Speed Control Strategy

In an indirect speed controller (ISC), the controller strategy is based on maximizing the power output by following a predefined maximum power curve which consists of taking as the electromagnetic torque reference T_{em}^* related to the maximum Power curve for each turbine rotational speed value

Ω_m using the dynamically stable nature of the VSWT around this curve. But the relationship between T_{em} and Ω_m has no dynamics this leads to a fixed soft response of the system. (Abad, G. & Lopez Taberna,2011; Pozo, Adrián & Ayala, Edy,2021) [38] and [39]

From the simulation of C_p as a function of λ and β , we can determine $C_{p,max}$ and λ_{opt} which will be useful to design the algorithm to follow the MPPT. In the following, we will focus on developing a strategy that allows us to determine the optimal electromagnetic torque applied to the generator shaft which mathematically and physically influences the mechanical rotation speed in an indirect way, so to have the MPPT, we must determine the optimal reference electromagnetic torque.

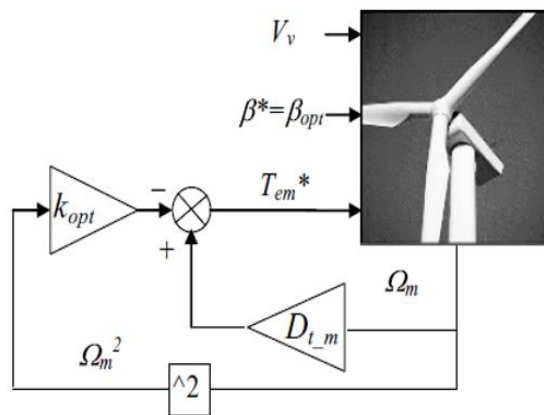


Figure.5 Indirect Speed Control strategy general block diagram

When the turbine is operating on the maximum power point:

$$\lambda_{opt} = \frac{R \Omega_t}{v_v}, \quad C_p = C_{pmax}, \quad \text{and} \quad T_t = T_{t-opt} \quad (10)$$

The turbine power harnessed from aerodynamic torque is therefore given by:

$$T_{t-opt} = \frac{1}{2} \rho \pi R^3 \frac{R^2 \Omega_t^2 C_{pmax}}{\lambda_{opt}^2 \lambda_{opt}}$$

$$T_{t-opt} = \frac{1}{2} \rho \pi \frac{R^5}{\lambda_{opt}^3} C_{pmax} \Omega_t^2 = K_{opt} \Omega_t^2 \quad (11)$$

Where

$$K_{opt} = \frac{1}{2} \rho \pi \frac{R^5}{\lambda_{opt}^3} C_{pmax}$$

It leads to an optimal torque that varies as a quadratic function of the wind turbine speed. Furthermore, from Equation (7) in the steady state:

$$0 = \frac{T_{t-ar}}{N} - D_t \Omega_{t-ar} N - K_{tm} (\Omega_{t-ar} - \Omega_m) \quad (12)$$

$$0 = T_{em} - D_m \Omega_m - K_{tm} (\Omega_{t-ar} - \Omega_m)$$

Where $\Omega_m = N \Omega_t$

$$T_{em} = -\frac{T_t}{N} + (D_m + D_t) \Omega_m \quad (13)$$

Substituting T_{t-opt} in Equation (11) with the expression from Equation (9), we have:

$$T_{em} = -K_{opt} \Omega_m^2 + (D_m + D_t) \Omega_m \quad (14)$$

Where

$$K_{opt} = \frac{1}{2} \rho \pi \frac{R^5}{\lambda_{opt}^3 N^3} C_{pmax} \quad (15)$$

The MPPT approach aims to enhance the efficiency of the Wind Energy Conversion System (WECS) by capturing the maximum possible power from the wind. To have the MPPT, it is necessary to determine the optimal electromagnetic torque so for each value of the wind speed and from the relation (15) we can determine Ω_t as well as Ω_m^* and from the relation (14) we can calculate the value of the corresponding reference torque T_{em}^* .

$$\Omega_t = \lambda_{opt} \frac{v_v}{R} \quad (16)$$

The reference electromagnetic torque, T_{em-ref}^* generated by the MPPT control strategy, ensures that the rotational speed is controlled around its reference value, Ω_{m-ref}^* , derived from Equation (16). This T_{em-ref}^* is then used as an input for the inner loop control structure. The proposed ANN-based MPPT controller is detailed in the next section.

Table1: Parameters for MPPT strategy

Parameter	Value	Description
Cp-max	0.479	Maximum power coefficient
Air density	1.225	Air density (kg/m ³)
λ_{opt}	8.2	Optimal Speed Ratio
R	40	Blade length (m)

N	90	Gearbox ratio
V_v	Input variable	Historical data of wind speed (m/s)
T_{em}^*	Output variable	Reference electromagnetic torque (Nm)
Ω_m^*	Input variable	Reference rotational speed (rad/s)
β_{opt}	0°	Optimal pitch angle
K_{opt}	$1.847256480310799e+05$	Aerodynamic constant
D_m	0.01	friction coefficient (Nms/(rad))
J_t	127	Inertia (kg m ²)

IV. ANN-based MPPT

Artificial Neural Network is a set of artificial neurons connected in layers, which work together to make predictions or classifications by adjusting its connections (weights) during training. The mathematical model of the neuron in lth layer is expressed as:

$$Y_j^l = f\left(\sum_{i=0}^{nl} W_{ji}^l X_i + b_j^l\right) \quad (17)$$

Where:

The inputs vector is X_i acquired through outputs of other neuron, W_{ji}^l designates the synaptic weights of neuron j in layer l, and b_j^l represents the bias input usually takes the value +1 or -1 in order to make the network more efficient as it learns because the tripping level of the neuron will change by adjusting weights and biases in learning.

The proposed MPPT neural controller is designed as a static Multilayer neural network (MLP). The architecture of the MLP used is illustrated in Fig. 6.

Multilayer neural network (MLP), or Multilayer Perceptron, is a type of artificial neural network used mainly in supervised learning tasks. Its structure is composed of several layers of neurons connected to each other by weights that are adjustable during training. (B. Deepa Lakshmi, & K. Sujatha, 2016; D. Fang, & J. Wang, 2017)[40] and [41]. MLP consisting of Input Layers which receives the raw input data (feature vectors). Each neuron in this layer represents an input variable and hidden Layers (one or more layers located between the input layer and the output layer). These layers are responsible for extracting complex features using nonlinear transformations. Each neuron in a layer is connected to the neurons in the previous and next layer and Output Layers which produce the prediction or classification based on the activations of the neurons in the last hidden layer.

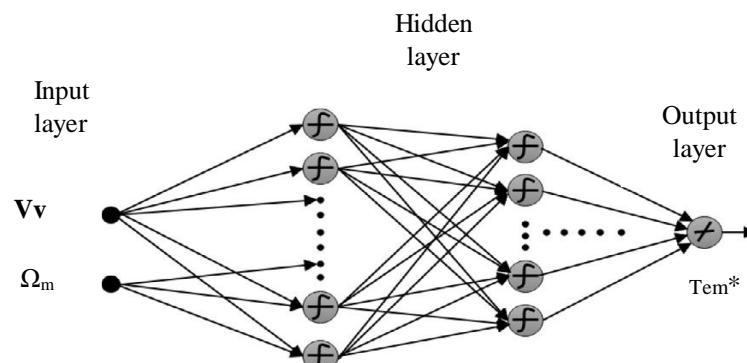


Figure.6 Internal structure of the MLP

This MLP consists of an input layer with two neurons representing wind speed V_v and mechanical speed Ω_m , two hidden layers, and an output layer with one neuron representing the **electromagnetic reference torque** $T_{em_ref}^*$. The hidden layers use hyperbolic sigmoid activation functions while the output neuron uses a linear activation

function and the MLP of **mechanical reference speed** Ω_m^* consists of an input layer with one neuron representing wind speed V_w and output layer with one neuron representing Ω_{mref} :

$$sgm = \frac{1 - \exp(-2x)}{1 + \exp(-2x)} \quad (18)$$

The collected data were divided into three subsets: 70% for training, 15% for testing, and 15% for validation. The training process of the MLP ($T_{em_ref}^*$ and Ω_m^*), depicted in fig.7a and fig7.b with MATLAB Simulink toolbox employed the Levenberg-Marquardt algorithm, known for its fast convergence and robustness. The number of iterations was set to 1000

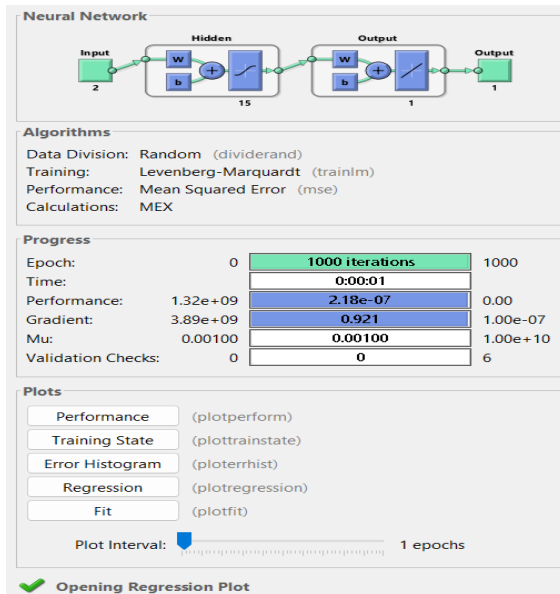


Figure7a. Neural Network Training of T_{em}^*

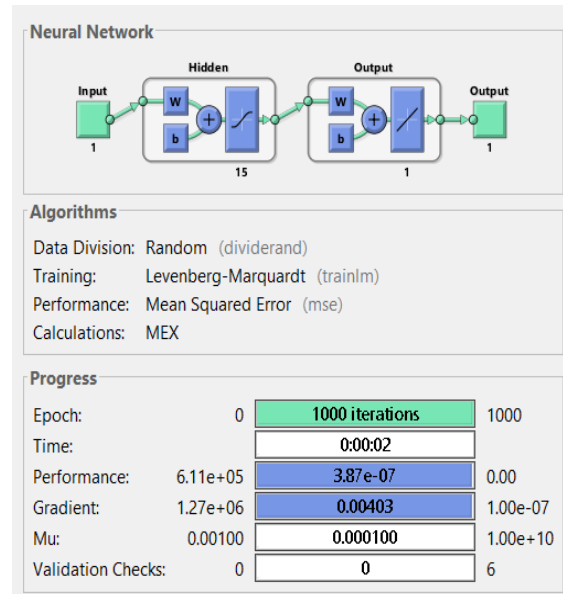


Figure.7b Neural Network Training of Ω_m^*

Figure 8 and Figure 9 illustrates that the proposed structure of $T_{em_ref}^*$ converged rapidly to an optimal solution, with only minor error variations observed thereafter, achieving an error rate of 5.2974×10^{-7} at epoch 1000 and for Ω_m^* (fig.10) the error rate of 3.7759×10^{-7} at epoch 1000.

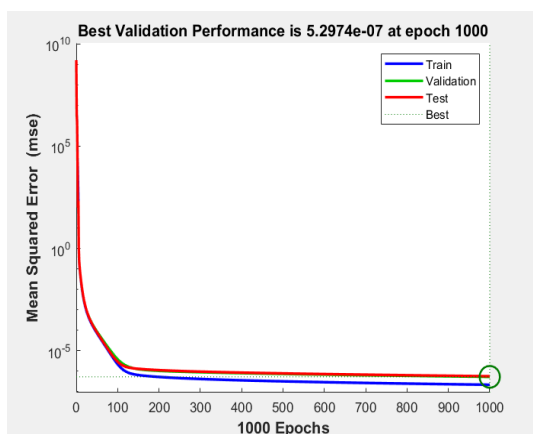


Figure.8 Performance curve of training T_{em}^*

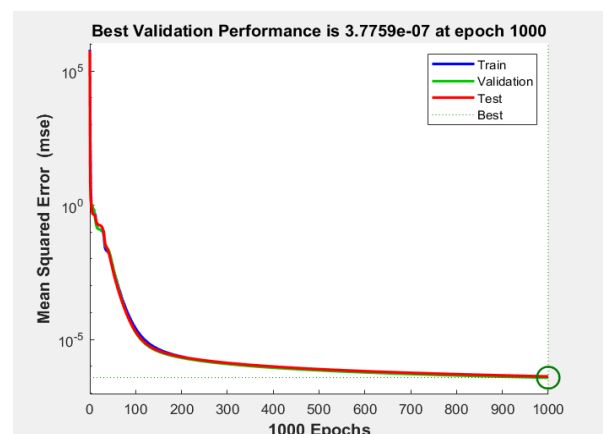


Figure.9 Performance curve of training Ω_m^*

In this part we have developed a reference electromagnetic torque T_{em}^* and a reference mechanical rotation speed

Ω_m^* using a neural network with a maximum power extracted using the MPPT algorithm. T_{em}^* and Ω_m^* will be useful later in the design of a sliding mode control robust to uncertainties and variations of parameters and external disturbances because the ISC approach leads to a close coupling between the electromagnetic torque T_{em} and the rotational speed Ω_m , as their relationship lacks the dynamic flexibility typically provided by a regulator.

in the method way we can determine the reference turbine torque T_t^* as well as the reference turbine power P_t^* using a neural network by referring to equations (5) and (11) we obtain:

$$P_{t\ opt} = T_{t\ opt}\Omega_t = K_{opt}\ \Omega_t^3 \quad (19)$$

The generator power given by:

$$P_{gen} = T_{em}\Omega_m \quad (20)$$

V. Sliding Mode Control design

In this section an ANN sliding mode controller (ANN-SMC) applied to the mechanical part of a 2 MW wind turbine based in figure 10. the objective is to ensure fast dynamic decoupling and robustness against external disturbances, allowing the wind turbine to quickly follow the reference values of rotation speed and electromagnetic torque obtained by ANN-MPPT.

The application of SMC for the regulation of Ω_m in a wind turbine system, where the MPPT (maximum power point tracking) imposes a nonlinear relationship between Ω_m and T_{em} , can significantly improve the speed of the response compared to a PI controller. Indeed, the goal is to manage dynamic couplings, ensure a fast response, maintain robustness against disturbances and product the optimal electrical energy. Many studies were proposed in this context (Kelkoul and Boumediene, 2021; Yao et al.,2021; H. Chojaa, A. Derouich,2021; B. Fatnassi and B. Torchani,2022; Torchani et al,2024)[42], [43], [44] and [45].

Sliding Mode Control Law for the System with above relation (7), the goal is to set Ω_m to track a desired reference corresponding to the MPPT (Maximum Power Tracking Point), aiming to extract maximum wind energy.

V.1. Classical sliding mode controller

a. Sliding Surfaces:

$$S_{\Omega_m} = \Omega_{m-ref} - \Omega_m \quad (21)$$

To determine the control law, it is necessary to determine the derivative of the sliding surface $\dot{S}(\Omega_m)$ which corresponds to:

$$\dot{S}(\Omega_m) = \frac{d\Omega_{m-ref}}{dt} - \frac{d\Omega_m}{dt} \quad (22)$$

The derivative of the reference is assumed to be known, to determine the derivative of Ω_m , we use equation (8) in equation (20) we obtain:

$$\dot{S}(\Omega_m) = \frac{d\Omega_{m-ref}}{dt} - \frac{1}{J_m} (T_{em} - D_m\Omega_m) \quad (23)$$

b. SMC control law:

The objective is to design a control law for T_{em} such that \dot{S}_{Ω_m} is always directed towards S_{Ω_m} . the system remains on the sliding surface:

$$S_{\Omega_m} = \dot{S}_{\Omega_m} = 0 \quad (24)$$

V.2. Calculation of the equivalent command:

The equivalent control is defined to maintain $\Omega_{m-ref} = \Omega_m$ while exactly compensating for dynamic effects:

$$T_{em-ref} = J_m \frac{d\Omega_{m-ref}}{dt} + D_m \Omega_{m-ref} \quad (25)$$

Using equation (21) to verify (22) with $S_{\Omega_m} = 0$, a typical SMC control law for the electromagnetic torque is given by:

The sliding mode control law is given by:

$$U_{eq} = T_{em-eq} = T_{em-ref} - K_{\Omega_m} \text{sgn}(S_{\Omega_m}) \quad (26)$$

- K_{Ω_m} : a command gain
- $-K_{\Omega_m} \text{sgn}(S_{\Omega_m})$: is the switching term that ensures that the system remains on the surface $S_{\Omega_m} = 0$

Using a Lyapunov function to verify this control law which guarantees convergence and ensures stability we will have:

$$V = \frac{1}{2} (S_{\Omega_m})^2 \quad (27)$$

VI. Convergence condition

The convergence condition is defined by the Lyapunov equation (25), it makes the surface attractive and invariant. The time derivative of the Lyapunov function must be defined negative to ensure stability, we will show that $\dot{V} < 0$

$$\dot{V} = \dot{S}_{\Omega_m} \cdot S_{\Omega_m} \quad (28)$$

By applying control law (24) in equation (21) and taking into account equation (23) we obtain:

$$\dot{S}_{\Omega_m} = -\frac{K_{\Omega_m} \text{sgn}(S_{\Omega_m})}{J_m} \quad (29)$$

By substituting this expression (27) in (26) we will have:

$$\dot{V} = -\frac{K_{\Omega_m}}{J_m} \text{sgn}(S_{\Omega_m}) S_{\Omega_m} = -\frac{K_{\Omega_m}}{J_m} |S_{\Omega_m}| \quad (30)$$

Or $\frac{K_{\Omega_m}}{J_m} > 0$ we clearly see that $\dot{V} < 0$ which means that V is decreasing, consequently S_{Ω_m} converges to 0 then the Lyapunov condition is satisfied.

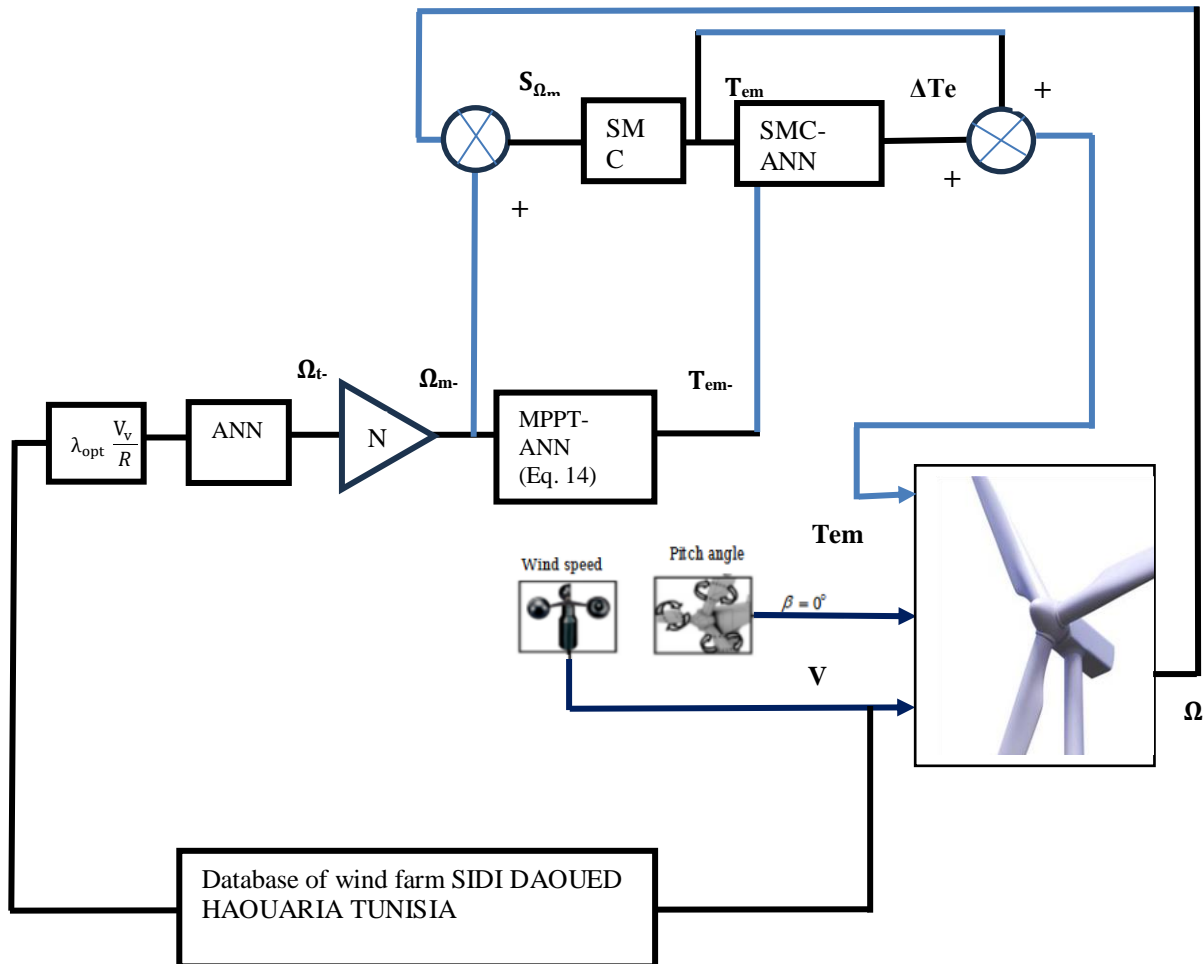


Figure. 10 General structure of control

V.2. ANN SMC

Sliding mode control coupled with an artificial neural network is a hybrid approach arising from the robustness of sliding mode control and the learning capabilities of the artificial neural network. Sliding mode control exhibits high robustness in the presence of parametric uncertainties or external perturbations due to the use of a sliding surface that provides stability by forcing the system to reach and stay on this surface. However, SMC often suffers from chattering, an undesirable oscillating motion caused by the discontinuous nature of the control. In order to overcome this defect, the sliding surface component is hybridized with a neural network to produce a smoother approximation of the control law. This increases the reference tracking accuracy while reducing oscillations. Therefore, SMC ANN proves to be an advanced and effective method for the control of complex systems such as wind turbine.

So, to avoid the chattering phenomenon related to the classical sliding mode control, we propose a hybrid control strategy that combines the classical SMC with the neural network tool so we will design a compensation command that provided by the neural network to smooth the command and reduce the chattering the neural network is used to adjust the dynamics of the gains according to the error $S_{\Omega_{m-}}$ and possibly its derivatives. Then the new command becomes:

$$T_{em} = T_{em-ref} + ANN(S_{\Omega_m}) \quad (31)$$

ANN(S_{Ω_m}):the output of the trained neural network to minimize the amplitude of S_{Ω_m}

The neural network acts as an adaptive and intelligent correction by learning from system dynamics and control data, it adjusts T_{em} in real time to minimize S_{Ω_m}

• **Neural network architecture**

Variable	Description	Dimensions
Inputs	Ω_m, S_{Ω_m}	2×1
Outputs	T_{em}	2×1

Simple network: Feedforward network (MLP) withone hidden layer (15 neurons).

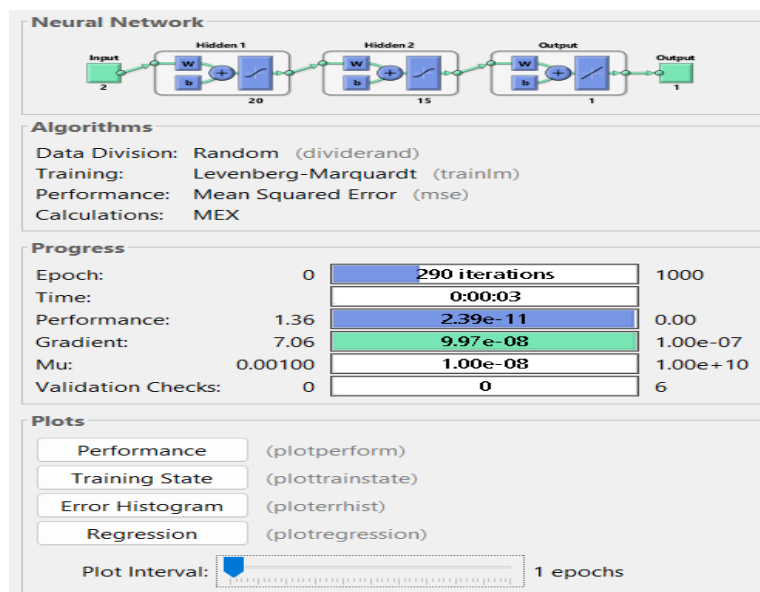


Figure.11 Neural Network Training of ΔT_{em} turbulent wind

The learning of ANN vector selector needs 290 iterations to reach a performance of $2.39 \cdot 10^{-11}$ within very short time, it takes only 0.3s.

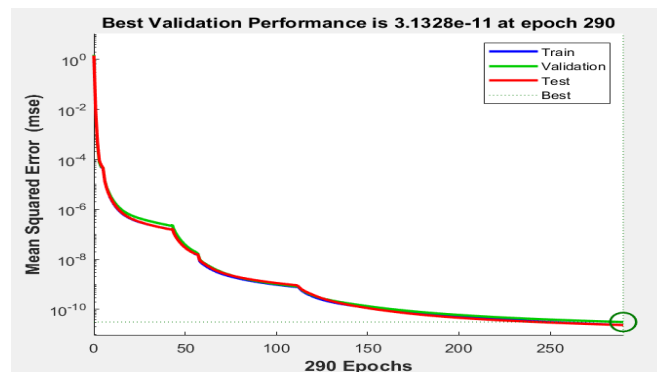


Figure.12 Performance curve of training ΔT_{em} with

VII. Simulation Results and Discussions

Table2: Simulation Parameters.

Parameter	Value
k_smc_ann	10
k_smc	13000
T_sim	10
u_smc	-3.730668943198770e+04
u_smc_ann	-2.09306855413555e+03
dt	0.01

In order to verify the performance of the proposed control, a simulation test will be conducted in Matlab/simulink software by using a 2 MW wind turbine. The parameters of turbine system are listed in Table 1 and the simulation parameters are given in Table 2. The assessment will be carried out on three wind variations: constant, turbulent, and gusty. The wind speed variations observed in different profiles observed in **figure 14**, (a) steady, (b) turbulent, and (c) gusty effectively illustrate the fluctuations throughout the simulation period. The steady wind profile, depicted as a constant 12 m/s line, serves as a reference point for evaluating system performance under stable conditions. Meanwhile, the turbulent profile, with its irregular oscillations, demonstrates peaks and dips that mimic real-world atmospheric behavior, underscoring the necessity of robust control strategies. On the other hand, the gusty profile, marked by sudden surges in wind speed, highlights the challenges these abrupt changes pose to the system's stability and efficiency. Collectively, these wind profiles offer critical insights into system performance under diverse conditions, reinforcing the importance of precise wind modeling for optimizing wind turbine operation.

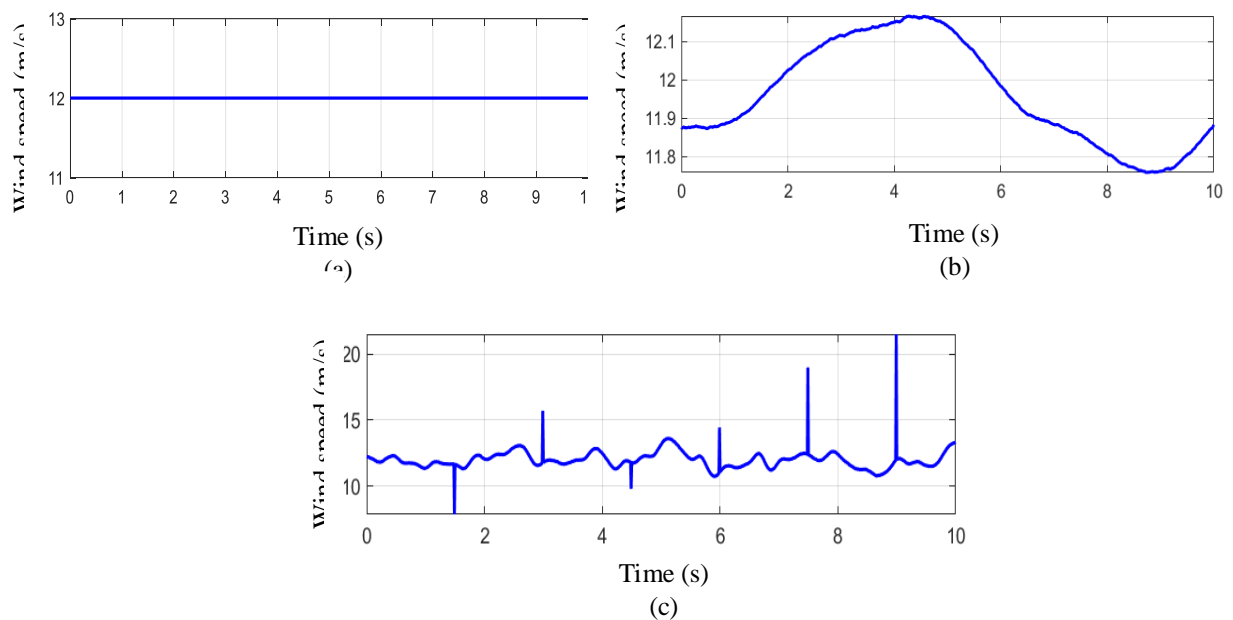


Figure.14 Wind speed profile of 12m/s mean value, (a) constant wind, (b) turbulent wind, (c) gusty wind.

Figure 15 illustrates the mechanical speed (Ω_m) of the wind turbine obtained using the proposed classical SMC and SMC-ANN controller under constant, turbulent, and gusty wind conditions. with classical SMC control, the figure reveals fluctuations appear at the beginning of the signals in Figures (a), (b), and (c), but they dissipate quickly about 0.05s. The control demonstrates smooth behavior, although the SMC controller exhibits a chattering

effect. Additionally, sudden variations due to wind gusts, particularly in figure 14(c), are noticeable with this type of control. However, the SMC-ANN effectively mitigates these fluctuations. Moreover, the SMC-ANN outperforms the conventional SMC, as evidenced by a minimal overshoot, and reduced tracking error without any chattering phenomenon. The representation of the sliding surface directly corresponds to the rotational error. A proper convergence toward this surface signifies that the system accurately follows the desired setpoint which is illustrated by **figure 16**. **Figure 17** shows the evolution of the electromagnetic torque (T_{em}) following its reference generated by MPPT strategy, as presented in these figures (a), (b) and (c) the torque curve coincides with the reference for the SMC ANN control but with classic SMC we can observe a shift this reflects a chattering phenomenon linked to the classic sliding mode control. We observe initially minor oscillations that quickly fade away after 0.04 seconds. Following this, the system responses track their references steadily under constant wind conditions. However, when gusts of wind occur, slight oscillations reappear, aligning with the gust intervals around 1.5s and 3s seconds. Overall, the SMC-ANN controller effectively suppresses these oscillations, ensuring accurate tracking with minimal errors and it has managed to reject the additive input disturbance. So, the SMC-ANN controller shows a better performance when compared with the classical SMC controller.

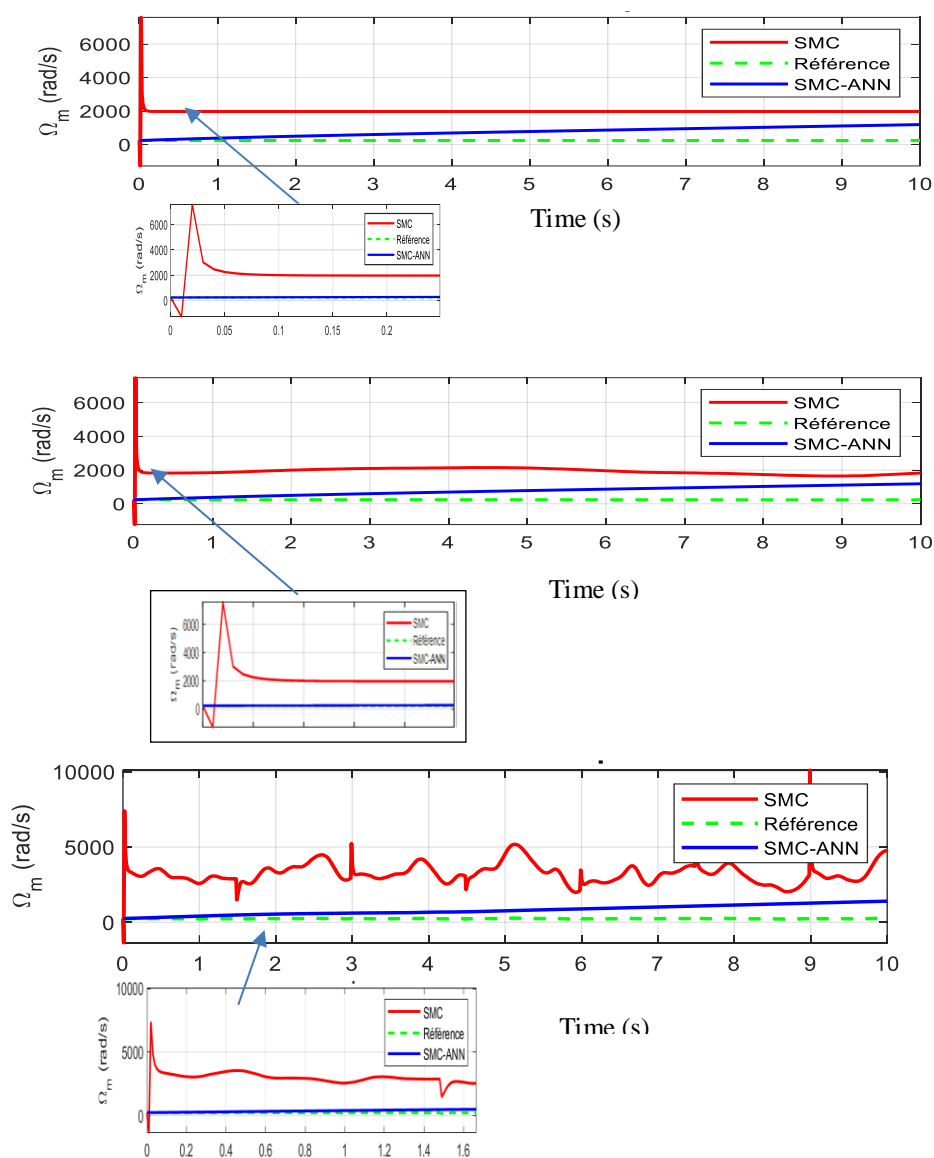


Figure.15 Mechanical speed of the proposed

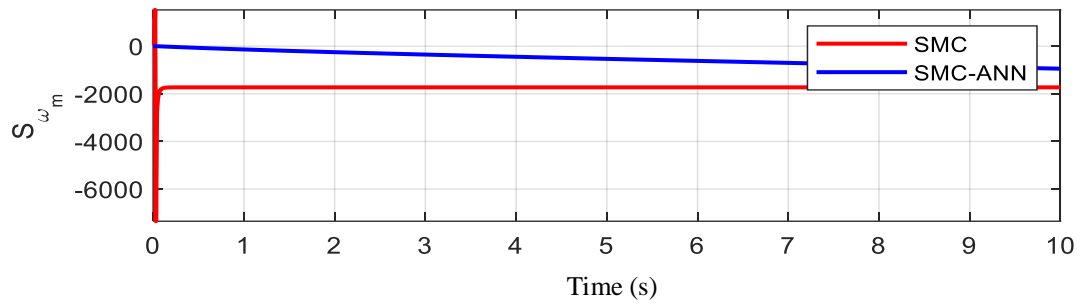
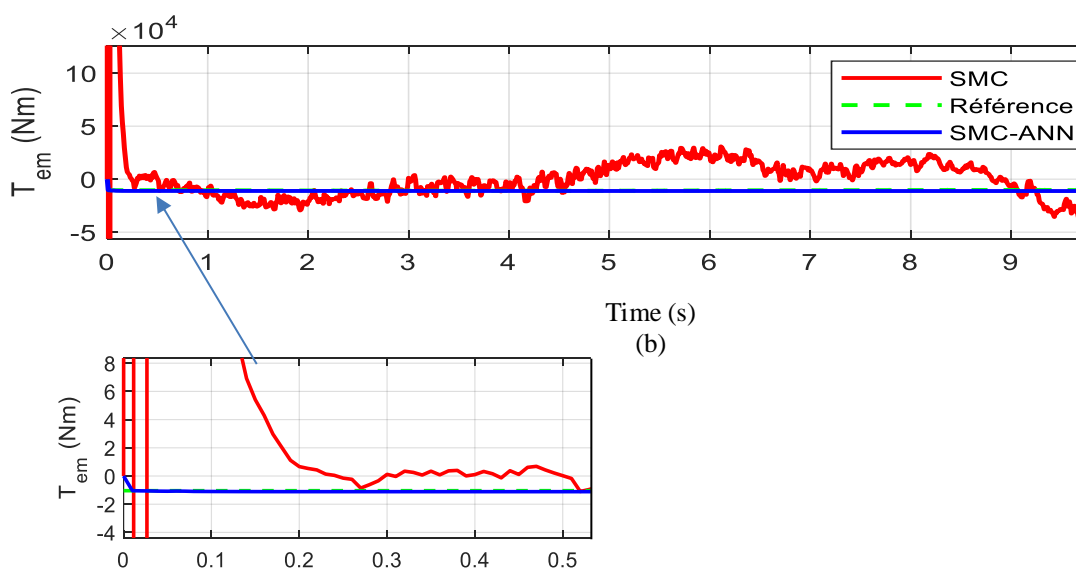
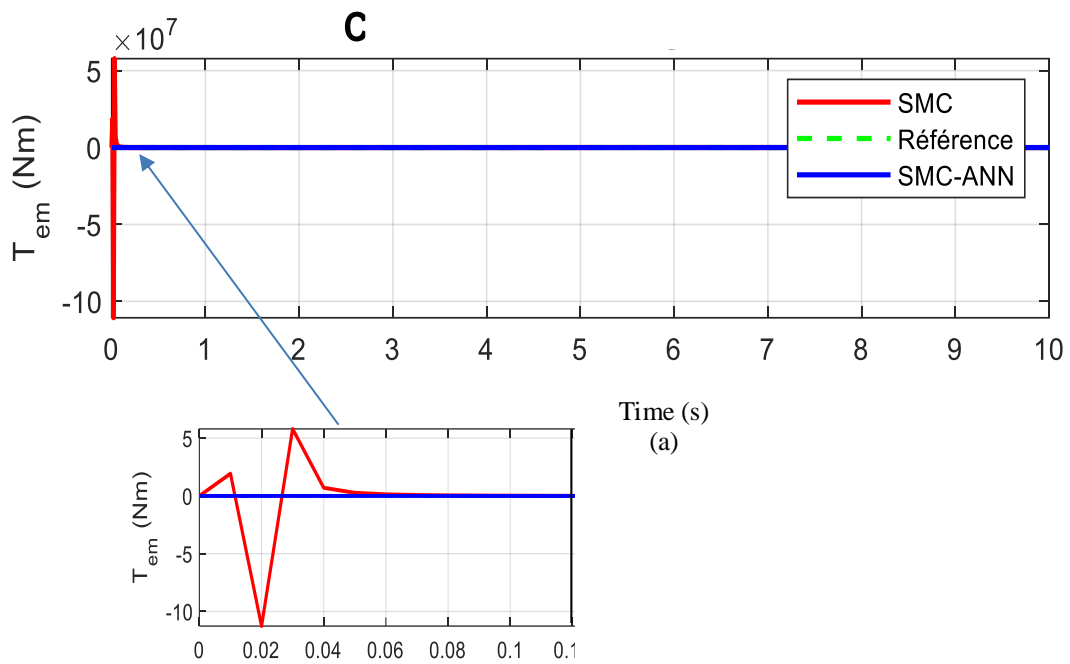


Figure.16 Sliding surface defining the rotation error.



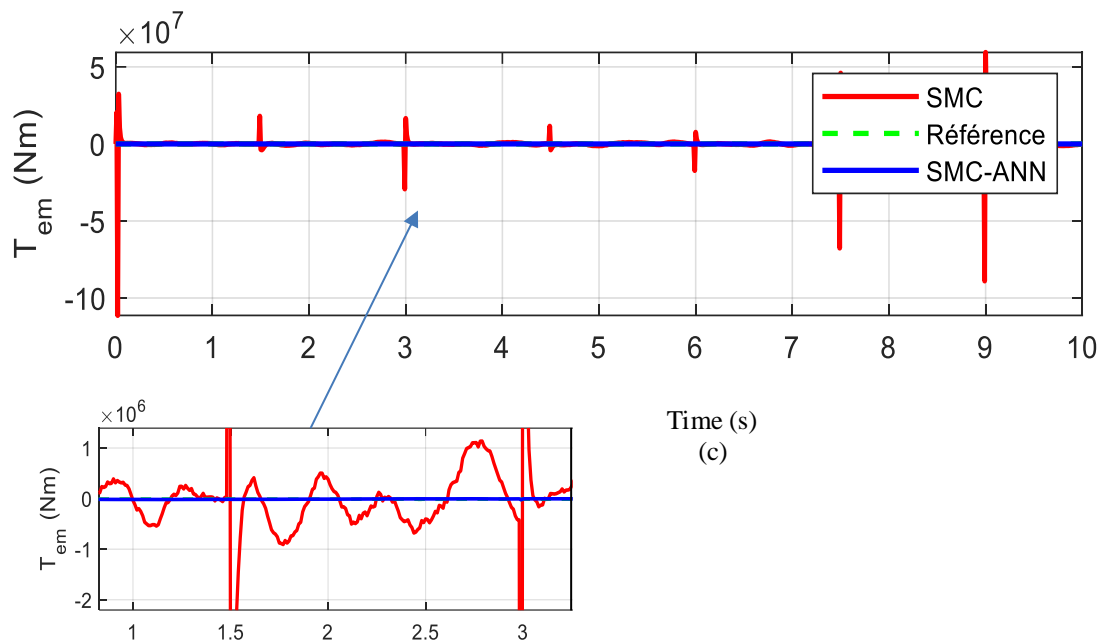
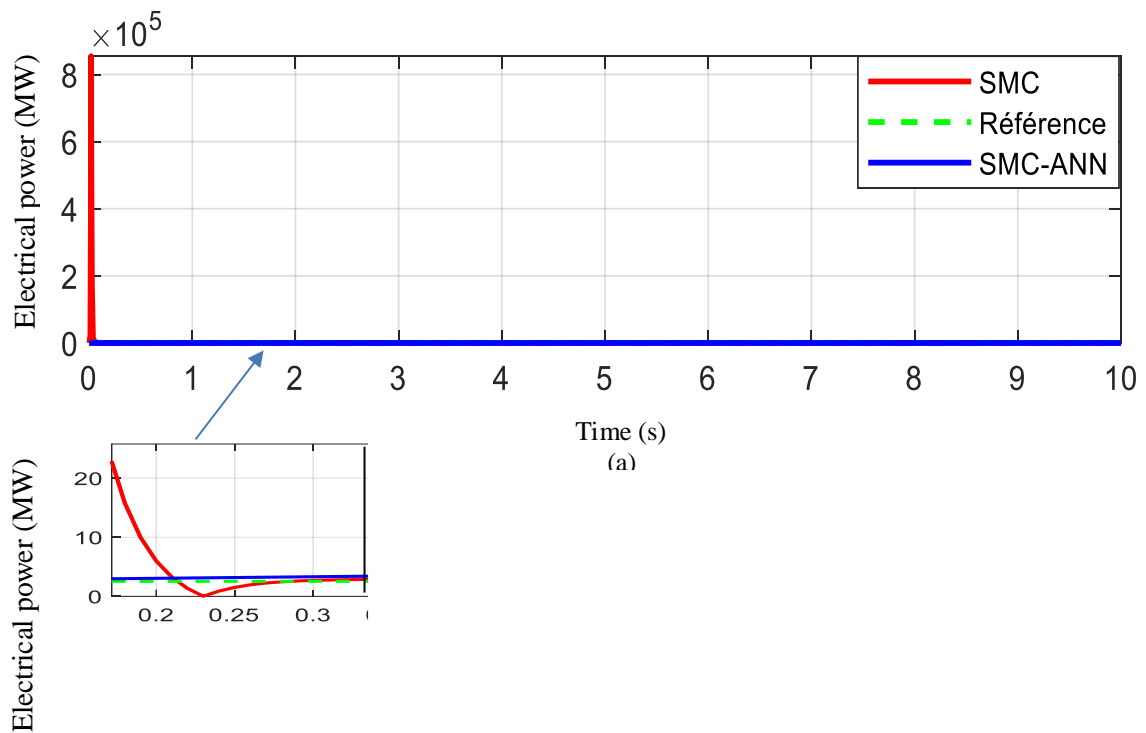


Figure.17 Electromagnetic torque (T_{em}) of the proposed methods: SMC and SMC-ANN, (a) constant wind, (b) turbulent wind, (c) gusty wind.



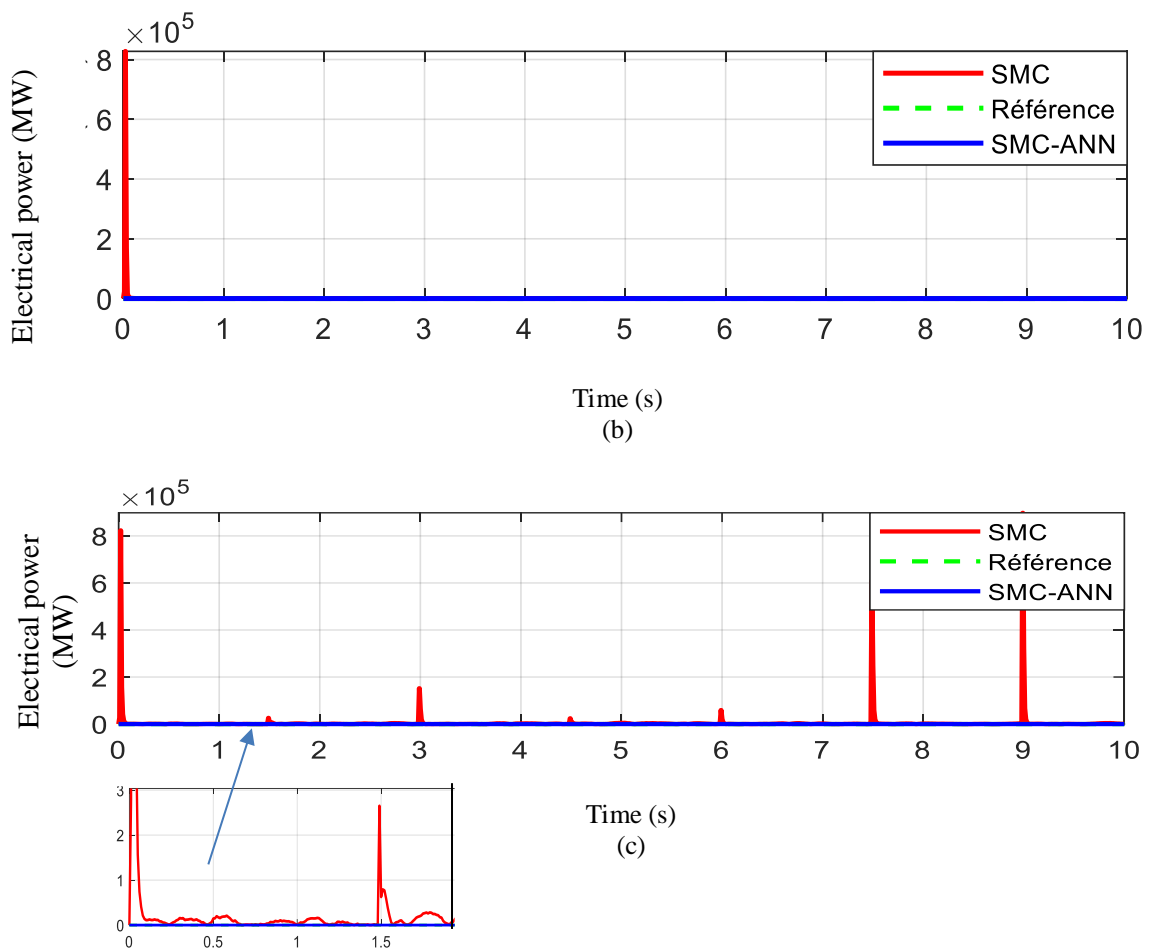


Figure.18 Electrical power (P_{gen}) of the proposed methods: SMC and SMC-ANN, (a) constant wind, (b) turbulent wind, (c) gusty wind.

As indicated in figure 18 (c), with the SMC-ANN controller of the electrical power avoid the tracking of the short – time turbulence (gust of wind) while the SMC controller is unable to reject the additive input disturbance at instants 1.5s, 3s, 7s and 9s. In figures 18 (a) and (b) the behavior of the two graphs shows a good convergence especially for the SMC- ANN control we notice that the signals follow their references.

The comparison of classical SMC yet to SMC_ANN is shown in Table 3. Here remarkable gains were achieved by both strategy control in terme of response time: The time is found when the error is less than 1.6842% of the reference. Those enhancements involve aovershoot, RMSE andsteady – state error of 0.536 for SMC-ANN controller

Table3: Comparison between SMC and SMC-ANN

Metric	SMC	SMC-ANN
Overshoot (%)	2.98	0.398
RMSE (rad/s)	1.701	0.601
Steady state error(rad/s)	1.684	0.536

The RMS error for SMC-ANN is low (0.601), this means that the difference between the actual values and the desired values is small, indicating that the system is accurate and tracks the reference well.

VIII. Conclusion

This paper presented an intelligent sliding mode control (SMC) integrated with maximum power point tracking (MPPT) and an indirect speed controller strategy to optimize the performance of mechanical wind turbine systems. The proposed control strategy effectively addressed challenges associated with variable wind speeds and nonlinear dynamics of wind turbine systems, ensuring efficient energy capture and system stability.

The simulation results demonstrated that the intelligent SMC-ANN strategy outperformed conventional control methods in terms of tracking accuracy, response time, and robustness against disturbances so this controller has succeeded in improving the decoupling between T_{em} and Ω_m . This approach provides a promising solution for improving the efficiency and reliability of wind energy systems, making it a valuable contribution to the renewable energy sector.

Acknowledgements

I am pleased to share that my paper has been officially accepted for publication by the Algerian Journal of Renewable Energy and Sustainable Development. I extend my sincere gratitude to the research team of ENSIT, LISIER Laboratory Tunis

References

- [1] Fatnassi B, Torchani A, Sellami A and Garcia G "Sliding mode control of DFIG for a variable speed wind turbine," IEEE International Conference on Control, Automation and Diagnosis (ICCAD), pp.1-5, 2022. DOI: 10.1109/ICCAD55197.2022.9854007
- [2] Steevens .C A and Flect N A 2004 Script Mater. 50 1335
- [3] Yeh M K, Cheng Y C and Wang C H 2015 Finite element stress analysis of wind blade structure under wind pressure. Taiwan Wind Energy Conference, Taipei, Taiwan, Paper No. SI_07 (in Chinese)
- [4] Meng-Kao Yeh and Chen-Hsu Wang, Stress analysis of composite wind turbine blade by finite element method, 5th conference ACMME, 2017 IOP Conf. Ser.: Mater. Sci. Eng. 241 012015 DOI 10.1088/1757-899X/241/1/012015
- [5] A. E. Yyaakoubi, A. Asselman, et K. Attari, « Adaptive State Feedback Pitch Angle Control of Wind Turbines for Speed Regulation and Blades Loadings Alleviation », Int. Rev. Autom. Control IREACO, vol. 11, no 4, p. 174-187, 2018, doi: 10.15866/ireaco.v11i4.14503.
- [6] EL YAAKOUBI, ALI & Amhaimar, Lahcen. (2022). Contrôle optimal de l'angle de calage des pales pour limiter la puissance produite et réduire les charges mécaniques des aéro- turbines. 84. 2022.
- [7] A.D. Wright, L. Fingersh, Advanced Control Design for Wind Turbines; Part I: Control Design, Implementation, and Initial Tests, Tech. Rep., National Renewable Energy Lab. (NREL), Golden, CO (United States), 2008.
- [8] Ahmad M. Wind Energy. Operation and Control of Renewable Energy Systems. John Wiley & Sons, Ltd; 2017:153-177.
- [9] Zhang X, Jia J, Zheng L, Yi W, Zhang Z. Maximum Power Point Tracking Algorithms for Wind Power Generation System: Review, Comparison and Analysis. Energy Sci Eng. 2023; 11: 430-444. doi:10.1002/ese3.1313
- [10] Xie, Jingjie & Dong, Hongyang & Zhao, Xiaowei. (2023). Data-driven torque and pitch control of wind turbines via reinforcement learning. Renewable Energy. <https://doi.org/10.1016/j.renene.2023.06.014>

- [11] Cardenas R, Pena R. Sensorless vector control of induction machines for variable-speed wind energy applications. *IEEE Trans Energy Convers.* 2004;19(1):196-205.
- [12] Datta R, Ranganathan VT. A method of tracking the peakpower points for a variable speed wind energy conversionsystem. *IEEE Trans Energy Conversion.* 2003;18(1):163-168.
- [13] H.Mousa, A.Youssef, E.Mohamed, State of the art perturb and observe MPPT algorithms based wind energy conversion systems: A technology review, *International Journal of Electrical Power & Energy Systems*, Volume 126, Part A, 2021, 106598, ISSN 0142-0615, <https://doi.org/10.1016/j.ijepes.2020.106598>.
- [14] Morimoto S, Nakayama H, Sanada M, Takeda Y. Sensorlessoutput maximization control for variable-speed wind genera-tion system using IPMSG. *IEEE Trans Ind Appl.* 2005;41(1):60-67
- [15] Koutroulis E, Kalaitzakis K. Design of a maximum powertracking system for wind-energy-conversion applications. *IEEE Trans Ind Electron.* 2006;53(2):486-494.
- [16] Hussein M, Senjyu T, Orabi M, Wahab M, Hamada M. Control of a Stand-Alone variable speed wind energy supply system. *Appl Sci-Basel.* 2013;3(2):437-456.58.
- [17] Martyanov AS, Troickiy AO, Korobotov SV. Performanceassessment of perturbation and observation algorithm for wind turbine. *International Conference on Industrial Engi-neering, Applications and Manufacturing (ICIEAM)*; 2018:1-5.
- [18] Wang Q, Chang L. An intelligent maximum powerextraction algorithm for inverter-based variable speed windturbine systems. *IEEE Trans Power Electron.* 2004;19(5):1242-1249
- [19] Hong MK, Lee HH. Adaptive maximum power point trackingalgorithm for variable speed wind power systems. *ICSEE 2010,LSMS 2010.* 2010:380-388
- [20] Kazmi SMR, Goto H, Guo HJ, Ichinokura O. A novelalgorithm for fast and efficient speed-sensorless maximumpower point tracking in wind energy conversion systems. *IEEE Trans Ind Electron.* 2011;58(1):29-36.
- [21] You X, Zhou B, Zuo GJ, Guo HH. A novel algorithm for fastand adaptive maximum power point tracking of windenergy generation system. *Adv Mater Res.* 2012;383-390:3633-3638.68.
- [22] Li, B.; Tang, W.; Xiahou, K.; Wu, Q. Development of Novel Robust Regulator for Maximum Wind Energy Extraction Based upon Perturbation and Observation. *Energies* 2017, 10, 569. <https://doi.org/10.3390/en10040569>
- [23] Pande, J.; Nasikkar, P.; Kotecha, K.; Varadarajan, V. A Review of Maximum Power Point Tracking Algorithms for Wind Energy Conversion Systems. *J. Mar. Sci. Eng.* 2021, 9, 1187. <https://doi.org/10.3390/jmse9111187>
- [24] Pucci M, Cirrincione M. Neural MPPT control of windgenerators with induction machines without speed sensors. *IEEE Trans Ind Electron.* 2011;58(1):37-47DOI: 10.1109/TIE.2010.2043043
- [25] A.E. Yaakoubi, L. Amhaimar, K. Attari, M.H. Harrak, M.E. Halaoui, A. Asselman, Non-linear and intelligent maximum power point tracking strategies for small size wind turbines: Performance analysis and comparison, *Energy Reports* , Volume 5, 2019, ISSN 2352-4847, <https://doi.org/10.1016/j.egyr.2019.03.001>
- [26] Ammar, H. H., Azar, A. T., Shalaby, R., and Mahmoud, M. I. (2019). Metaheuristic optimization of fractional order incremental conductance (FO-INC) maximum power point tracking (MPPT). *Complexity* 2019, 1–13. doi.org/10.1155/2019/7687891
- [27] Berrada, Y., and Boumhidi, I. (2020). New structure of sliding mode control for variable speed wind turbine. *IFAC J. Syst. Control* 14, 100113. doi.org/10.1007/978-981-13-1945-7_13
- [28] H.Chojaa, A.Derouich, S.Chehaidia, O.Zamzoum, M. Taoussi, H. Elouatouat, Integral sliding mode control for DFIG based WECS with MPPT based on artificial neural network under a real wind profile, *Energy Reports*, Volume 7, 2021, Pages 4809-4824, ISSN 2352-4847, doi.org/10.1016/j.egyr.2021.07.066
- [29] Bu-Lai W, Zi-Xin L, Ye-Cheng L, Jing-Heng Z (2023) Fuzzy sliding mode control of PMSM based on PSO. *IEICE Electron Express* 20(20):20230346. doi.org/10.1587/elex.20.20230346

- [30] Padmanabhuni, Nishanth & Pieper, Jeff. (2023). First Order Dynamic Sliding Mode Control of a Wind Turbine with Optimized Tip Speed, The 10th International Conference of Control, Dynamic Systems, and Robotics Ratio. 10.11159/cdsr23.217. DOI:10.11159/cdsr23.217
- [31] T. Borhen , A. A. Taher , A. Saim , M. A.Redha , K. I. Ibraheem, „Sliding mode control based on maximum power point tracking for dynamics of wind turbine, system,Frontiers in Energy Research, volume12, 2024 ISSN-296-598 <https://doi.org/10.3389/fenrg.2024.1434695>
- [32] Slotine, J.-J. E., Hedrick, J. K., and Misawa, E. A. (1986). “On sliding observers for nonlinear systems,” in 1986 American control conference, Seattle, WA, USA, 1794–1800.
- [33] Itkis, U. (1976). Control systems of variable structures. New York: Wiley
- [34] Slotine, J.-J. E., and Hong, S. (1986). “Two-time scale sliding control of manipulators with flexible joints,” in 1986 American control conference, Seattle, WA, USA, 805–810.
- [35] Yashar Mousavi, Geraint Bevan, Ibrahim Beklan Kucukdemiral, Afef Fekih, Sliding mode control of wind energy conversion systems: Trends and applications, Renewable and Sustainable Energy Reviews, Volum167, 2022,112734, ISSN 1364-0321,doi.org/10.1016/j.rser.2022.112734
- [36] Zheng, X., Li, L., Xu, D., and Platts, J. (2009) “Sliding mode MPPT control of variable speed wind power system,” in 2009 asia-pacific power and energy engineering conference, 1–4.
- [37] Freris, L. L. (1990). Wind energy conversion systems. Englewood Cliffs, NJ: PrenticeHall, 182–184.
- [38] Pozo, Adrián & Ayala, Edy & Simani, Silvio & Muñoz Palomeque, Eduardo. (2021). Indirect Speed Control Strategy for Maximum Power Point Tracking of the DFIG Wind Turbine System. Revista Técnica Energía. 17. 92-101. 10.37116/revistaenergia.v17.n2.2021.426. DOI:10.37116/revistaenergia.v17.n2.2021.426
- [39] Abad, G. & Lopez Taberna, Jesus & Rodriguez, Miguel & Marroyo, Luis & Iwanski, Grzegorz. (2011). Doubly Fed Induction Machine: Modeling and Control for Wind Energy Generation. 10.1002/9781118104965. DOI:10.1002/9781118104965
- [40] B. Deepa Lakshmi, & K. Sujatha (2016) “Artificial neural networks for wind speed prediction.” International Journal of Control Theory and Applications9 (4): 1953-1959
- [41] D. Fang, & J. Wang (2017). A novel application of artificial neural network for wind speed estimation.” International Journal of Sustainable Energy36 (5): 415-429. DOI:10.1080/14786451.2015.1026906
- [42] B. Fatnassi, B. Torchani, A. Sellami and G. Garcia, "Behavior of DFIG Based Wind Turbine During Symmetric Dips with Crowbar and Sliding Mode Control Solution," 2023 IEEE Third International Conference on Signal, Control and Communication (SCC), Hammamet, Tunisia, 2023, pp. 1-5, DOI: 10.1109/SCC59637.2023.10527603
- [43] Yao, M., Xiao, X., Tian, Y., and Cui, H. (2021). A fast terminal sliding mode control scheme with time-varying sliding mode surfaces. J. Frankl. Inst.358 (10), 5386–5407. doi.org/10.1016/j.jfranklin.2021.05.006
- [44] Kelkoul, B., and Boumediene, A. (2021). Stability analysis and study between classical sliding mode control (SMC) and super twisting algorithm (STA) for doubly fed induction generator (DFIG) under wind turbine.Energy214,118871.doi.org/10.1016/j.energy.2020.118871
- [45] V. Petrović, M. Jelavić, et M. Baotić, « Advanced control algorithms for reduction of wind turbine structural loads », Renew. Energy, vol. 76, p. 418-431, avr. 2015, doi: 10.1016/j.renene.2014.11.051.
- [46] Martin, N., Talens-Peiró, L., Villalba-Méndez, G., Nebot-Medina, R., and MadridLópez, C. (2023). An energy future beyond climate neutrality: comprehensive evaluations of transition pathways. Appl. Energy 331 (1), 120366. doi:10.1016/j.apenergy.2022.120366B.
- [47] L. Fan, R. Kavasseri, Z. L. Miao and C. Zhu, "Modeling of DFIG-Based Wind Farms for SSR Analysis," in IEEE Transactions on Power Delivery, vol. 25, no. 4, pp. 2073-2082, Oct. 2010, doi: 10.1109/TPWRD.2010.2050912.

- [48] Yang, J., Li, N., and Wang, X. (2017). Optimal power control for wind turbine system based on the simplified fuzzy-PID controller. *Int. J. Power Eng. Eng. Thermophys.* 1 (1), 1–10. doi:10.23977/poweet.2017.11001
- [49] Lalouni, S., Rekioua, D., Idjdarene, K., & Tounzi, A. (2015). Maximum Power Point Tracking Based Hybrid Hill-climb Search Method Applied to Wind Energy Conversion System. *Electric Power Components and Systems*, 43(8–10), 1028–1038. doi.org/10.1080/15325008.2014.999143
- [50] González-Hernández JG, Salas-Cabrera R. Maximum powercoefficient analysis in wind energy conversion systems:questioning, findings, and new perspective. *Math Prob Eng.*2021;2021:9932841-9932847
- [51] Chehaidia, S.E., Abderezzak, A., Kherfane, H., Boukhezzar, B., Cherif, H., 2020a.An improved machine learning techniques fusion algorithm for controlsadvanced research turbine (Cart) power coefficient estimation. *UPB Sci. Bull. C* 82, 279–292.
- [52] Jiao, X., Yang, Q., Fan, B., Chen, Q., Sun, Y., and Wang, L. (2020). EWSE and uncertainty and disturbance estimator based pitch angle control for wind turbine systems operating in above-rated wind speed region. *J. Dyn. Syst. Meas. Control* 142 (3), 031006. <https://doi.org/10.1115/1.4045561>
- [53] Frikh, M. L., Soltani, F., Bensiali, N., Boutasseta, N., and Fergani, N. (2021). Fractional order PID controller design for wind turbine systems using analytical and computational tuning approaches. *Comput. Electr. Eng.* 95, 107410. doi:10.1016/j.compeleceng.2021.107410
- [54] C. Wei, Z. Zhang, W. Qiao and L. Qu, "Reinforcement-Learning-Based Intelligent Maximum Power Point Tracking Control for Wind Energy Conversion Systems," in *IEEE Transactions on Industrial Electronics*, vol. 62, no. 10, pp. 6360-6370, Oct. 2015, doi.org/10.1109/TPEL.2016.2514370
- [55] Chen J, Cai K, Lin T, et al. Adaptive maximum power pointtracking control strategy for variable-speed wind energyconversion systems with constant tracking speed. 2019 22ndInternational Conference on Electrical Machines and Systems(ICEMS). 2019:1-5
- [56] Hui J, Bakhshai A, Jain PK, et al. An adaptive approximationmethod for maximum power point tracking (MPPT) in windenergy systems. 2011 IEEE Energy Conversion Congress andExposition. 2011:2664-2669.69.
- [57] Trinh Q-N Lee H-H Fuzzy logic controller for maximum power tracking in PMSG-based wind power systems BT-advanced intelligent computing theories and applications. With aspects of artificial intelligence 2010 543 553 doi.org/10.1007/978-3-642-14932-0_68
- [58] Lisitsyn, A. N., and Zadorozhnaya, N. M. (2019). Adaptive wind turbine PID controller tuner algorithm with elements of artificial intelligence. *Procedia Comput. Sci.* 150, 591–596. doi:10.1016/j.procs.2019.02.098
- [59] Alqudah, A. (2020). Controlling of wind turbine generator system based on genetic fuzzy-PID controller. *Int. J. Adv. Trends Comput. Sci. Eng.* 9 (1), 409–425. doi:10.30534/ijatcse/2020/58912020
- [60] Jingjie Xie, Hongyang Dong, Xiaowei Zhao,Data-driven torque and pitch control of wind turbines via reinforcementlearning,*RenewableEnergy*, Volume215,2023,118893,ISSN09601481, <https://doi.org/10.1016/j.renene.2023.06.014>.